Morphology and Viscoelastic Properties of Polystyrene Blended with Fully Condensed Polyhedral Oligomeric Silsesquioxanes

Madhu Namani[1], Hai-Ping Geng[1(a)], Andre Lee[1*], Rusty L. Blanski[2]

[1]Department of Chemical Engineering and Materials Science
Michigan State University
E. Lansing, MI. 48824

[2]Air Force Research Laboratory
PRSM, Bldg. 8451, 10 E. Saturn Blvd.
Edwards AFB, CA. 93524-7680

[*] To Whom Correspondence should be addressed

[(a)] Presently at Beijing University of Chemical Technology

E-mail: leea@egr.msu.edu

<table>
<tr><td colspan="2"><h1>Report Documentation Page</h1></td><td>Form Approved
OMB No. 0704-0188</td></tr>
</table>

Report Documentation Page		*Form Approved* *OMB No. 0704-0188*

Public reporting burden for the collection of information is estimated to average 1 hour per response, including the time for reviewing instructions, searching existing data sources, gathering and maintaining the data needed, and completing and reviewing the collection of information. Send comments regarding this burden estimate or any other aspect of this collection of information, including suggestions for reducing this burden, to Washington Headquarters Services, Directorate for Information Operations and Reports, 1215 Jefferson Davis Highway, Suite 1204, Arlington VA 22202-4302. Respondents should be aware that notwithstanding any other provision of law, no person shall be subject to a penalty for failing to comply with a collection of information if it does not display a currently valid OMB control number.

1. REPORT DATE **18 OCT 2004**	2. REPORT TYPE	3. DATES COVERED **-**
4. TITLE AND SUBTITLE **Morphology and Viscoelastic Properties of Polystyrene Blended with Fully Condensed Polyhedral Oligomeric Silsesquioxanes**		5a. CONTRACT NUMBER
		5b. GRANT NUMBER
		5c. PROGRAM ELEMENT NUMBER
6. AUTHOR(S) **Madhu Namani; Hai-Ping Geng; Andre Lee; Rusty Blanski**		5d. PROJECT NUMBER **4847**
		5e. TASK NUMBER **0249**
		5f. WORK UNIT NUMBER
7. PERFORMING ORGANIZATION NAME(S) AND ADDRESS(ES) **Air Force Research Laboratory (AFMC),AFRL/PRSM,10 E. Saturn Blvd.,Edwards AFB,CA,93524-7680**		8. PERFORMING ORGANIZATION REPORT NUMBER
9. SPONSORING/MONITORING AGENCY NAME(S) AND ADDRESS(ES)		10. SPONSOR/MONITOR'S ACRONYM(S)
		11. SPONSOR/MONITOR'S REPORT NUMBER(S)
12. DISTRIBUTION/AVAILABILITY STATEMENT **Approved for public release; distribution unlimited**		
13. SUPPLEMENTARY NOTES		

14. ABSTRACT

Polyhedral oligomeric silsesquioxane (POSS) offers a unique approach to examine the effect of molecularly dispersed nanoscopic fillers on rheological properties of entangled polymer melts. Experiments were performed using a nearly-monodisperse molecular weight polystyrene (PS) blended with varying amounts of two fully condensed POSS molecules surrounded with phenethyl and styrenyl groups. Due to the chemical similarity between these organic moieties surrounding the silicon-oxygen framework ($SiO_{1.5}$) of POSS and PS, we were able to obtain polymer blends with molecular dispersed nanoscopic fillers needed to study the effect of intermolecular nanoparticle-nanoparticle interactions and the associated intramolecular interactions on the dynamics of the polymer chains. Differential Scanning Calorimetry (DSC) Wide-angle X-ray Diffraction (WAXD) and Transmission Electron Microscopy (TEM) were used to characterize the thermal properties and morphologies of the POSS/PS blends. Smallstrain oscillatory shear and/or tensile method was used to probe the dynamics of polymer chains as influenced by the addition of different chemical moiety of POSS at the glass transition rubbery state and the terminal-flow transition regions. Results obtained from the thermal and mechanical characterization methods were compared with morphological observations to better understand the structure-property relationship of polymers containing molecularly dispersed nanoscopic fillers.

15. SUBJECT TERMS					
16. SECURITY CLASSIFICATION OF:			17. LIMITATION OF ABSTRACT	18. NUMBER OF PAGES **37**	19a. NAME OF RESPONSIBLE PERSON
a. REPORT **unclassified**	b. ABSTRACT **unclassified**	c. THIS PAGE **unclassified**			

Abstract

Polyhedral oligomeric silsesquioxane (POSS) offers a unique approach to examine the effect of molecularly dispersed nanoscopic fillers on rheological properties of entangled polymer melts. Experiments were performed using a nearly-monodisperse molecular weight polystyrene (PS) blended with varying amounts of two fully condensed POSS molecules surrounded with phenethyl and styrenyl groups. Due to the chemical similarity between these organic moieties surrounding the silicon-oxygen framework ($SiO_{1.5}$) of POSS and PS, we were able to obtain polymer blends with molecular dispersed nanoscopic fillers needed to study the effect of intermolecular nanoparticle-nanoparticle interactions and the associated intramolecular interactions on the dynamics of the polymer chains. Differential Scanning Calorimetry (DSC), Wide-angle X-ray Diffraction (WAXD) and Transmission Electron Microscopy (TEM) were used to characterize the thermal properties and morphologies of the POSS/PS blends. Small-strain oscillatory shear and/or tensile method was used to probe the dynamics of polymer chains as influenced by the addition of different chemical moiety of POSS at the glass transition, rubbery state and the terminal-flow transition regions. Results obtained from the thermal and mechanical characterization methods were compared with morphological observations to better understand the structure-property relationship of polymers containing molecularly dispersed nanoscopic fillers.

Introduction

Demand for the continued advancement of performance and materials properties in polymeric and composite materials has driven the search for new technologies and methods for upgrading the properties of existing polymers. This search has in turn led to development of the field of nano-composites, which ultimately seeks to reinforce polymer chains at the molecular level in much the same way as fiber-reinforced composites at the macroscopic level.

Nano-reinforced plastics have their origins in the mid '80s with the use of sol-gel compounds to form homogeneous dispersions of inorganic domains throughout a polymeric matrix.[1] This approach has gained some commercial value in coating applications where its complex processing and limited materials strength are most easily tolerated. In the early '90s, the field saw the emergence of a second approach with the resurgence in the use of minerals and clay fillers that have been treated with various surfactants[2]. By selecting specific surfactant treatments and polymer combinations, the mineral or clay fillers can undergo intercalation or exfoliation with the polymers. The molecular dispersion of clay fillers in polymers often leads to significant mechanical and transport properties improvement at the rubbery state of these polymeric nano-composites. This approach is of considerable interest to many plastics compounders because of the strong tradition within the industry of using minerals and color pigments[3]. However, some drawbacks such as the degradation of surfactants during processing and high melt viscosity are limiting factors. In this paper, we present a third approach, the use of chemically well-defined Polyhedral Oligomeric Silsesquioxanes (POSS) as model nano-fillers, that can be blended into polymers and achieve dispersion at the molecular level.

A typical fully condensed T_8 POSS molecule is a well-defined cluster with a diameter range of 1 to 3 nm, and is represented by the formula $R_8Si_8O_{12}$ with an inorganic silica-like core

(Si_8O_{12}) surrounded by eight organic corner groups (R_8)[4]. Since the size of a single POSS molecule is in the range of 1 to 3 nm, it is similar to the molecular dimensions for segmental motions of a linear polymer. Therefore, in order to obtain an engineering solution for POSS based nano-composites, it is proposed to model polymers with molecularly-dispersed POSS as a mixture of a two-component system. As will be shown below, molecular dispersion can be achieved by controlling the compatibility between the organic group surrounding the inorganic silica-like core of POSS and polymer matrix.

The thermodynamic properties of a polymer (A) – nanoparticle (B) mixture can be best explained by Flory-Huggins theory, which can be expressed by as the following equation.

$$\Delta G_{mix} = RT(n_1 \ln \phi_1 + n_2 \ln \phi_2) + V_1(\delta_1 - \delta_2)^2 \phi_1 \phi_2$$

The terms in the above equation that describe the mixing behavior between two components, are V, the molar volume, δ, the solubility parameter, ϕ, the volume fraction and n, the mole fraction. To a first order approximation, the solubility parameters are determined using group contribution methods. To form a single phase mixture, the value of ΔG_{mix} must be less than zero. The first two terms that represent the entropy of arranging A and B are both negative. The third term is the interaction term and is positive; i.e. $(\delta_1 - \delta_2)^2$. Thus, for POSS, if the organic group surrounding the inorganic core is chemically similar to the polymer, it is likely the value of $(\delta_1 - \delta_2)$ is small. Thus a single phase mixture may be more favorable.

The interaction between two particles, which was first described by Asakura and Oosawa[5] and Vrij,[6] showed that there is an osmotic imbalance pushing the particles together if they are within a certain distance of each other. The interaction between colloidal spheres and

polymer molecules has been studied theoretically via a number of techniques: scaling approaches[7,8], field theory[9-12], computer simulation[13,14], integral equations[15,16] and other approaches[17-19]. In this paper we focus on the influence of interactions between POSS nanoparticles and polymers on the polymer chain dynamics.

Experimental

Materials: Nearly monodisperse molecular weight distribution of polystyrene with M_w= 290K Daltons (polydispersity less than 1.1) were purchased from Pressure Chemicals. Two fully condensed POSS molecules, Styrenyl$_8$-POSS (St$_8$T$_8$, **1**) and Phenethyl$_8$-POSS (Ph$_8$T$_8$, **2**), were used in this study. The chemical structures are illustrated below.
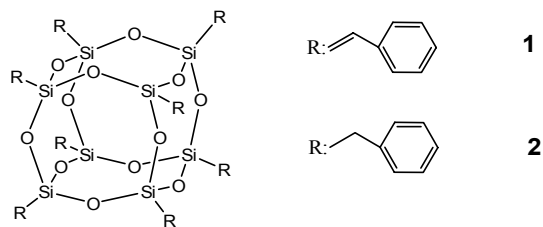
Synthesis of POSS: Degassed toluene (Fisher) was purified by elution through an alumina column. Grubbs Catalyst Cl$_2$Ru(=CHPh)(PCy$_3$)$_2$ (Strem) was used as received. Styrene (Aldrich) was purified by distillation under diminished pressure onto ~10 ppm of catechol. Hydrogen (Scott Specialty Gases) and 10% Palladium on Carbon (Aldrich) were used as received. All NMR spectra were collected on either a Bruker Avance 300 or 400 MHz spectrometer. ^{1}H, ^{13}C and ^{29}Si NMR spectra (reported in ppm using the δ scale) were referenced to residual CHCl$_3$ at 7.26 ppm, to CDCl$_3$ at 77.0 ppm, and to external SiMe$_4$ at 0 ppm, respectively.

Synthesis of Styrenyl$_8$T$_8$ (**1**): the following is a modification to the originally reported synthesis of **1**[20]: A 500 mL round bottom flask was charged with 15 grams (26.7 mmol, 189.5

mmol vinyl) of Vinyl$_8$T$_8$, 35mL (305 mmol) of Styrene, 50 mL of toluene and a stir bar under nitrogen. 200 mg (0.24 mmol) of the Cl$_2$Ru(=CHPh)(PCy$_3$)$_2$ (dissolved in 10 mL of toluene) was added to the reaction via syringe. A slight vacuum was applied to the flask to assist in the volatilization of ethylene that was generated in the process, and the mixture was allowed to stir overnight. The volatiles were removed under vacuum and redissolved in toluene. To this mixture was added 30 grams of montmorillonite clay and the mixture stirred for 45 minutes. The reaction was filtered through Celite, and the colorless filtrate was evaporated to give a colorless solid. This solid was heated under vacuum at 150ºC for two hours and then 100ºC overnight to remove any stilbene formed. 27 grams of **1** was obtained as an odorless, free flowing solid (92% yield).

Synthesis of Phenethyl$_8$T$_8$ (**2**): A 300 mL Parr reactor was charged with 20 grams of Styrenyl$_8$T$_8$, 50 mg of 10% palladium on carbon, and 30 mL of toluene. The reactor was pressurized to 500 psi of hydrogen and allowed to stir overnight at 50°C. The reaction was cooled to ambient temperature and the solution filtered through Celite. The volatiles were removed and the remaining liquid was heated to 150°C under vacuum for two hours. 19.5 grams of a colorless solid was obtained (97% yield). ^{1}H NMR (300.1 MHz, CDCl$_3$) δ 7.381 (m, 5H, C$_6$H$_5$), δ 2.904 (m, 2H, CH$_2$Ph), δ 1.152 (m, 2H, Si-CH$_2$). ^{13}C NMR (75.5 MHz, CDCl$_3$) δ 143.97, 128.32, 127.84, 125.74, 28.93, 13.73. ^{29}Si NMR (59.6 MHz, CDCl3) δ -67.2.

Sample Preparation:

Transmission Electron Microscopy: Transmission Electron Microscopy (TEM) images were obtained using a JEOL 100CX TEM using an acceleration voltage of 120 KV. PS and POSS were dissolved in THF at a concentration of 5 mg per ml of THF and stirred for more than 3 hours. The solution was then dropped onto a glass slide and let to dry in air. The film was

removed from the glass slide by slowly immersing the slide into a vessel of water at an angle of 45° to the surface. TEM grids were dropped onto the film, and the test assembly was lifted out of the water using a section of paper. The samples were dried on filter paper and subsequently carbon coated to increase their beam stability.

X-ray Diffraction: X-ray diffraction measurements were performed using a Scintag 2000 XRD with Cu-K$_\alpha$ target (λ=1.54Å) radiation generated at 45 kV and 200 mA. The diffraction angle was ranged from 5° to 30°, with step size and scan rate of 0.05^o and 2° per minute, respectively. POSS/PS blends were prepared by dissolving both POSS and PS chloroform and stirred for 12 hours with a magnetic stirrer. The mixture was poured onto a glass surface and covered with a slight gap to allow slow evaporation of solvent to form a thin polymer film. The as-cast film was dried in a vacuum oven for 24 hours at 60^oC.

Differential Scanning Calorimeter and Rheological Characterization: Preparations of POSS/PS blends were performed by dissolving PS and POSS macromers in chloroform and stirring the solution for 12 hours using a magnetic stirrer and crashing the sample out by using a bad solvent (methanol). The precipitated sample on crashing out of the solvent was filtered and then dried under vacuum for more than 12 hours at 60^oC.

Differential Scanning Calorimeter: Transition temperatures were determined using a Mettler-Toledo 821e/400 differential scanning calorimeter (DSC) under a flow of nitrogen and with a heating rate of 10^oC per minute. The transition temperature was taken as the inflection point of the transition region.

Melt Rheological Characterization: Rheological measurements were carried out using a Rheometric Scientific ARES-II rheometer equipped with a force convection oven in the parallel plate geometry. Parallel plate geometry with a diameter of 8 mm and a gap of 0.5 mm was used

for all measurements obtained in this study. Rheological behavior of all samples was investigated using a series of isothermal, small-strain oscillatory shear with oscillatory frequency ranging from 100 to 0.1 radian/second and oscillatory shear strain amplitude of 10%. To examine the validity of the time-temperature superposition principle and the effect of POSS addition on the values of time-temperature shift factor, the sample was tested at temperatures ranging from T_g+10^oC to T_g+100^oC with 10^oC intervals. Values of storage modulus, $G'(\omega)$, loss modulus, $G''(\omega)$, and damping factor, $\tan\delta(\omega) = G''(\omega)/G'(\omega)$, were determined using software provided by Rheometric Scientific. Samples tested under the same experimental conditions were repeated two to three times to confirm their reproducibility. Master curves for G', G'' and $\tan\delta$ were also obtained with a software package provided by Rheometric Scientific, and a reference temperature of $T_{ref}=150^oC$ for pure polymers and blends was used.

Thermo-Mechanical Analysis: POSS/PS solutions of varying POSS concentrations (0%, 6%, 13.3%, 20% and 30%) were made by dissolving PS (M_w= 290K Daltons) and POSS macromers in chloroform and stirring the solution for 12 hours using a magnetic stirrer. From this solution films were cast on a glass surface, allowing the solvent to evaporate out slowly at room temperature. The films were dried and annealed at 105^oC overnight in a vacuum oven to remove trace amounts of solvent and residual stress due to the solvent casting method.

Thermo-mechanical properties of PS/POSS films were analyzed using a Rheometric Scientific Solid Analyzer RSA III operated in a rectangular compression-tension mode. Samples used were in a shape of rectangular film strips with dimensions of $12\times 3 \times 0.2$ mm^3. The experiments were performed using an oscillatory frequency of 6.26 radians/second and oscillatory strain amplitude of 0.1%. All measurements were carried out from room temperature to 120^oC for all PS/POSS blends at a heating rate of 2^oC per minute.

Results and Discussion

Differential Scanning Calorimeter

Figures 1 and 2 depict DSC curves of Ph_8T_8 POSS, its blend with PS, St_8T_8 POSS and its blend with PS, respectively. As observed from these DSC curves, the value of heat of fusion for Ph_8T_8 and St_8T_8 POSS is nearly identical (~ 37.7 kJ/mole). In addition, for the case of 30 wt% POSS/PS blends, we did not observe any crystalline melting peaks associated with the pure POSS macromers, which suggests that POSS-PS blends form a single phase mixture. The melting transition temperature from the DSC measurement can be used to estimate the strength of associations within the POSS crystallites. As determined from the DSC, the onset of melting transition peak for St_8T_8 is around $274^{o}C$ and Ph_8T_8 was at $77^{o}C$. The higher transition temperature indicates a stronger POSS-POSS association in St_8T_8 as compared to Ph_8T_8.

DSC results were also used to examine the effect of the addition of POSS on the T_g of blends. Values of T_g as obtained by DSC are summarized in Table 1. For the case of PS blended with Ph_8T_8 POSS, the value of T_g decreased as the amount of POSS increased. However, the percentage of St_8T_8 in PS had almost no effect on T_g. We believe the suppression of T_g in the case of Ph_8T_8 blends was caused by the well-dispersed POSS clusters in PS and the excellent mutual solubility between Ph_8T_8 and PS, thereby causing a swelling in the polymer network, similar to that of solvent plasticization effect, which was further confirmed by rheological measurements. As for St_8T_8/PS blends, although the POSS may have been well dispersed, there was a lack of interaction between POSS and PS where the enthalpic contribution to the Gibb's free energy of mixing may be neglected. The blend may be treated as a well-dispersed, albeit inert, nano- particulate filled polymer.
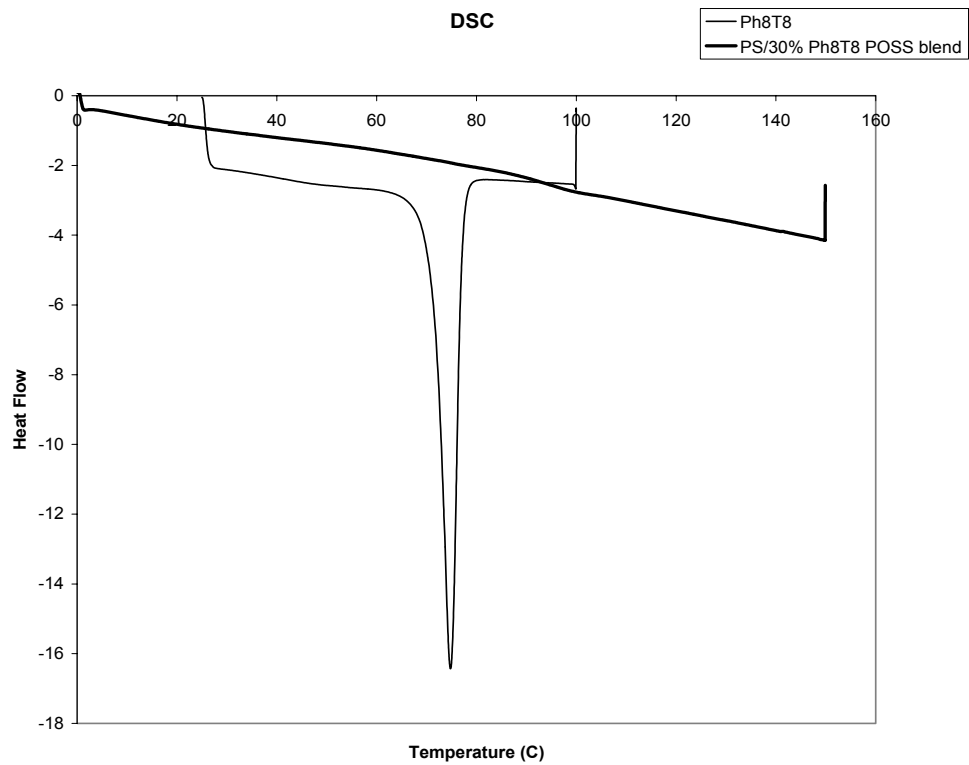
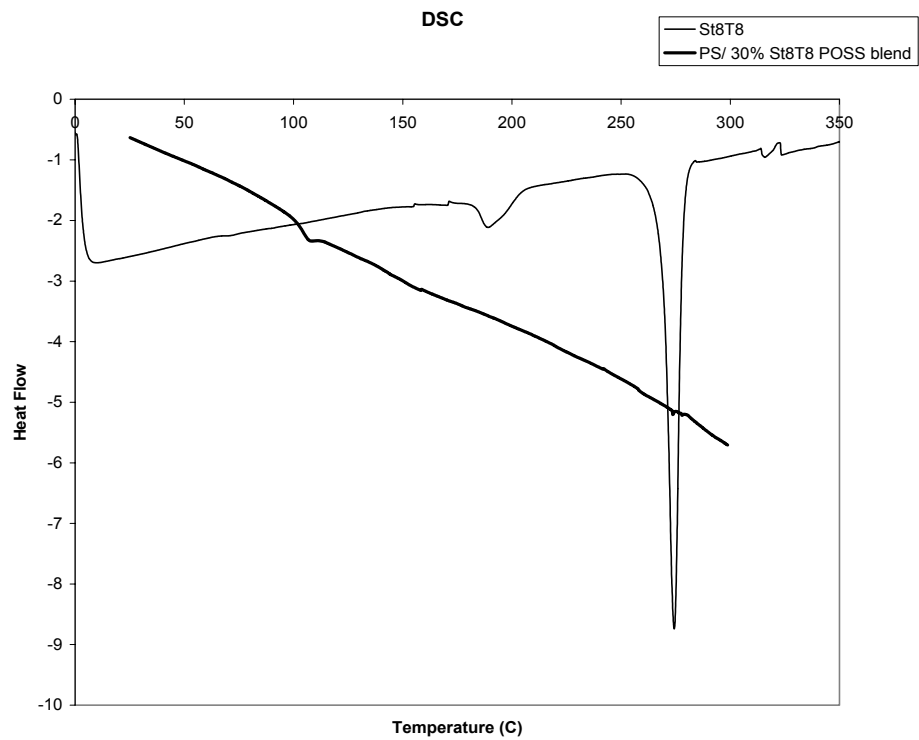Figure 1 DSC plot of Phenethyl POSS (Ph$_8$T$_8$) and PS (M$_W$= 290K Da) / Phenethyl POSS 30%wt blend

Figure 2 DSC plot of Styrenyl POSS (St_8T_8) and PS (M_W= 290K Da) /Styrenyl POSS 30%wt blend

Table 1

Summary of rheological data for blends investigated in this study. The polystyrene used here is a nearly-monodispersed molecular weight with M_w=290,000

	Φ	T_g	ω_C	$G_C(\omega)$	$\lim_{\omega \to 0} \eta^*(\omega)$	G_N^0
	wt %	°C	rad/s	Pa	Pa-s	Pa
PS 290K Pure		106.1	0.0182	4.18E+04	6.02E+06	2.35E+05
Ph8T8/PS						
	2%	102.2	0.0261	4.68E+04	4.51E+06	2.23E+05
	6%	100.7	0.0295	3.43E+04	2.98E+06	1.54E+05
	13.3%	101.4	0.0276	3.51E+04	3.58E+06	1.69E+05
	20%	98.6	0.0709	3.27E+04	1.19E+06	1.42E+05
	30%	91.9	0.1827	2.71E+04	3.77E+05	1.05E+05
	50%	N/A	N/A	N/A	N/A	3.68E+04
	70%	N/A	N/A	N/A	N/A	1.87E+04
	90%	N/A	N/A	N/A	N/A	3.00E+03
St8T8/PS	2%	105.4	0.0227	4.27E+04	4.27E+06	1.67E+05
	6%	104.7	0.0170	3.33E+04	3.33E+06	1.64E+05
	13.3%	104.9	0.0200	3.72E+04	3.72E+06	1.90E+05
	20%	105.8	0.0204	3.98E+04	3.98E+06	1.74E+05
	30%	103.7	0.0285	2.91E+04	2.91E+06	1.57E+05

Φ=*POSS* weight fraction is $\approx$ volume fraction since densities of both POSS and PS are approximately 1.

G_N^0 is the plateau modulus and is determined as the value of G' at minimum tanδ position.

T_g is determined as the midpoint of onset and end set of transition from the DSC curve.

ω_C is the crossover frequency and $G_C(\omega)$ is the modulus at the crossover frequency.

$\lim_{\omega \to 0} \eta^*(\omega)$ is the zero shear viscosity from the master curve at 150°C based on Ellis model.

N/A Not Available

Morphological Studies

Transmission Electron Microscopy (TEM) was utilized to characterize the morphologies of the POSS/PS blends, and X-ray diffraction was employed to identify the morphological changes of POSS macromers after they were blended with PS.

X-ray Diffraction:

The effects of the PS on the crystalline structures of POSS were studied by comparing the X-ray diffraction patterns of the POSS macromers in the POSS/PS blends with those of the neat POSS macromers. The results reflect the degree of compatibility between the POSS macromers and PS.

From Figures 3 and 4, it could be seen that the crystalline POSS peak in the case of PS blends containing 20 wt% of POSS disappeared for Ph_8T_8 and St_8T_8 respectively compared to the pure POSS macromers results, suggesting the high compatibility between the POSS macromers and PS. The disappearance of the crystalline POSS peak suggests that the POSS macromers are completely dispersed in the PS matrix.

Transmission Electron Microscopy:

The morphology of the PS/POSS blends was observed by using a Transmission Electron Microscope. These experiments were done to study the effects of different chemical moieties of POSS used and POSS loading on the morphological structures of the PS/POSS blends. A higher molecular weight PS was used to facilitate better mechanical properties to the film, especially since very dilute solutions were employed to cast the sample films.

Figures 5 and 6 depict the TEM photographs of PS (molecular weight 2M Daltons) blended with Ph_8T_8 POSS and St_8T_8 POSS, respectively. A high POSS loading (50 wt%) was
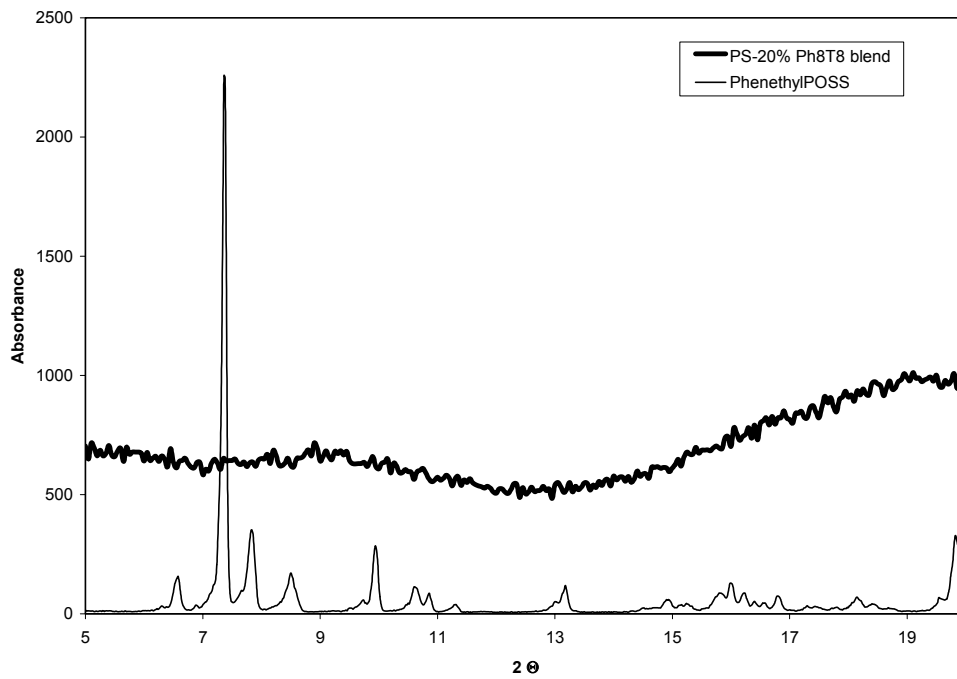
Figure 3 X-Ray plot of Phenethyl POSS (Ph$_8$T$_8$) and PS (M$_W$= 290K Da) / Phenethyl POSS 20%wt blend
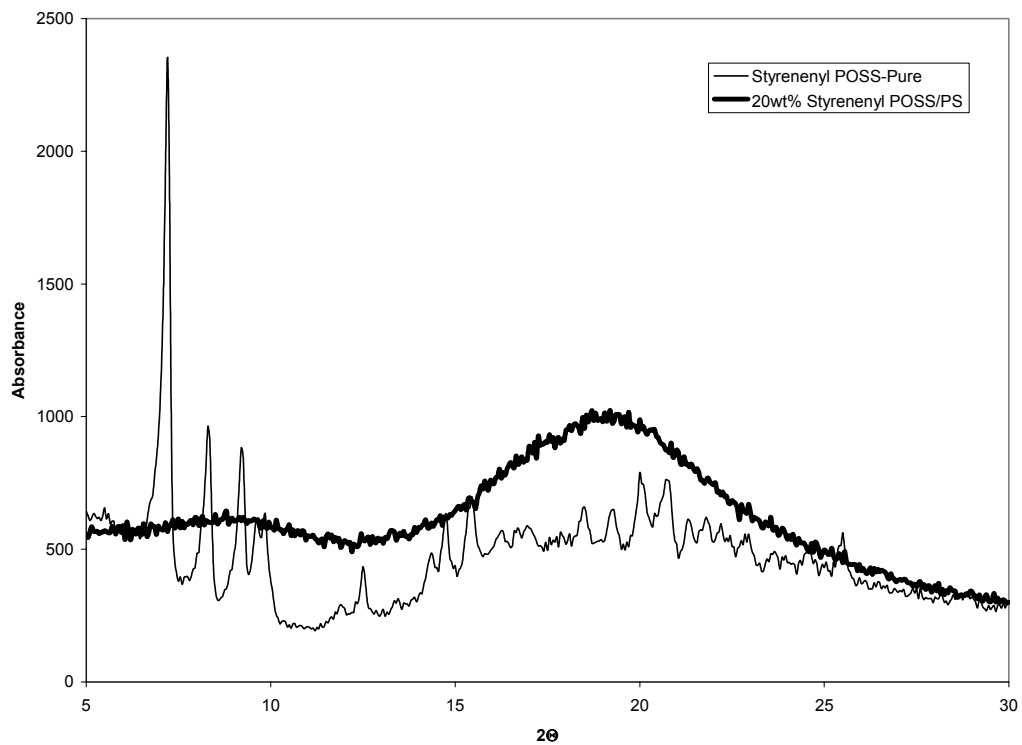
Figure 4 X-Ray plot of Styrenyl POSS (St_8T_8) and PS (M_W= 290K Da) /Styrenyl POSS 20%wt blend

used in this study to facilitate better contrast between the dispersed and the continuous phases; if any phase separation is observed. As can be seen from Figure 5, the Ph_8T_8 POSS macromer is homogeneously dispersed in the PS matrix. The substitution of phenethyl groups by the styrenyl groups on the POSS cages renders regions with different concentrations of POSS, as observed in Figure 6. The continuous phase has a higher concentration of POSS, while the dispersed phase appears to have lower concentration. This observation was further investigated by varying the loading of St_8T_8 in PS. In Figure 7, the POSS loading was decreased to 20 wt%. Similar phase behavior was observed to that of the 50 wt% blends, with the only difference being the decreased contrast of the dispersed phase in POSS/PS blends.

This decrease in the contrast of the polymer phase implies better diffusion of the St_8T_8 POSS macromers in the polymer phase. This is possible when the POSS phase dimension is lower, as in the 20% loading compared to that of the 50% loading due to less phase segregation, since concentration is a driving force for phase behavior.

Rheology:

Rubbery State and Flow Transition

The effect of POSS loading and distribution of POSS macromers in PS is understood through the thermal and morphological studies. Rheology experiments were performed to address the effect of POSS macromers on the chain dynamics of PS. Since rheological measurements and their correlation to polymer chain dynamics using narrow molecular weight PS properties were well documented, our measurements of POSS/PS blends will provide insight into how the POSS macromers affect the polymer chain dynamics.

The melt rheological experiments were carried out using small-strain amplitude oscillatory shear so to minimize deformation on sample morphology. The dynamic properties of
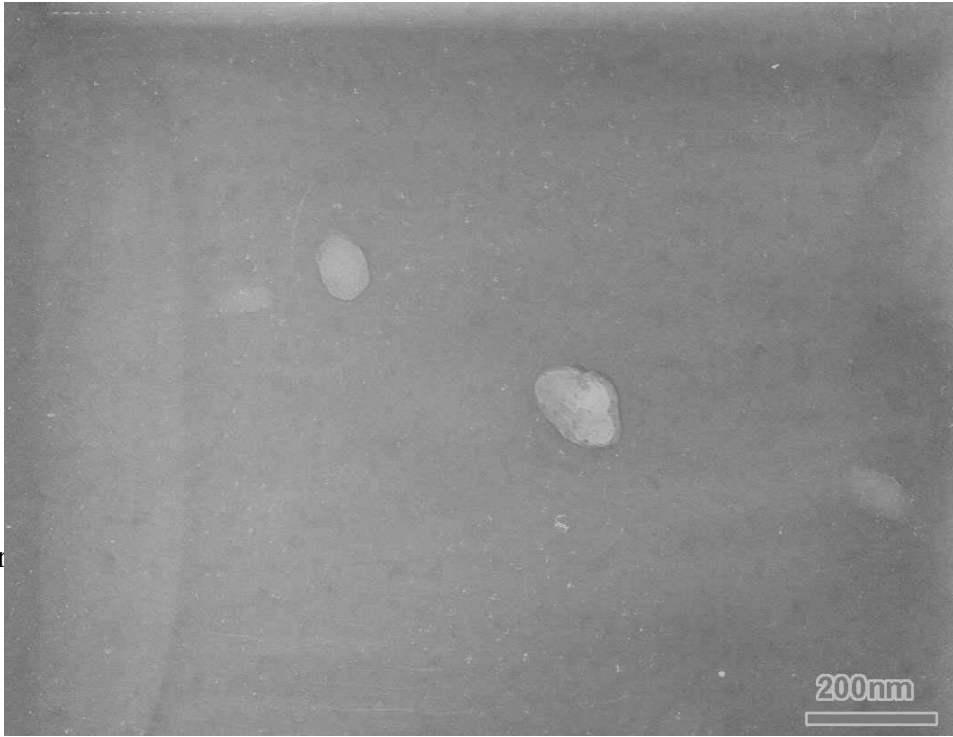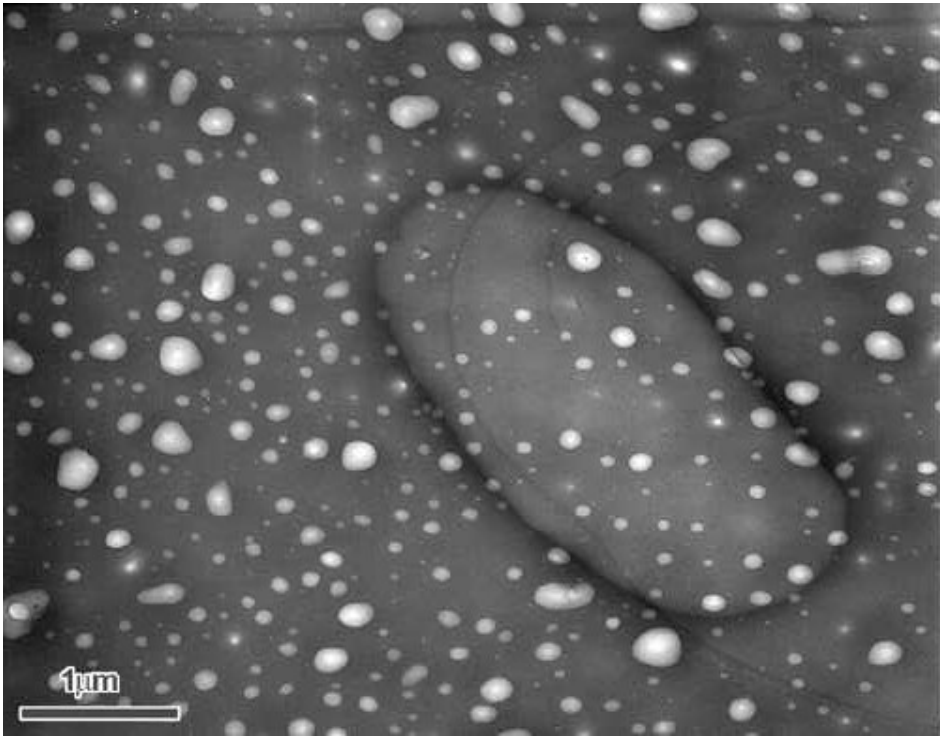
Figur   SS)

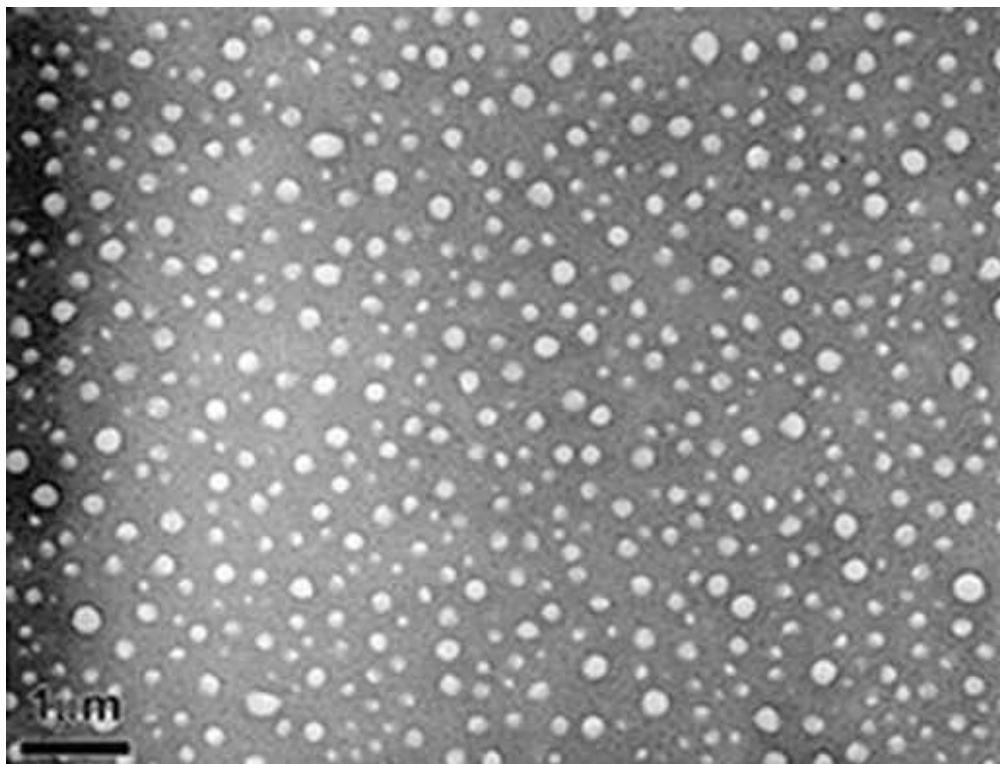Figure 6 TEM Image of PS (M_W= 2M Da)/ Styrenyl POSS blend (20 wt% POSS)

Figure 7 TEM Image of PS (M_W= 2M Da)/ Styrenyl POSS blend (50 wt% POSS)

the POSS/PS blends were investigated as a function of frequency at different temperatures.

Changes in $G_C(\omega)$, ω_C, G_N^0 and $\lim_{\omega \to 0} \eta^*(\omega)$ were compared for all studied systems. In addition, the validity of time-temperature superposition was also verified for all the samples used in this study.

Ph_8T_8 POSS / PS Blends

Figure 8(a) shows the time-temperature master curves shifted to $150^{\circ}C$ for the PS (Molecular weight 290K Daltons) blended with varying amounts of Ph_8T_8 POSS. The corresponding plot of reduced complex viscosity versus reduced frequency is shown in Figure 8(b). The temperature shift factor versus temperature is plotted in Figure 8(c). From the various reduced storage modulus curves shown in Figure 8(a), we observed that these curves shift downwards and towards the right with increasing amount of Ph_8T_8 POSS blended. In addition, the values of the plateau modulus, G_N^0, and the cross-over frequency, ω_C, as shown in Table 1, decrease with increasing amount of Ph_8T_8 POSS added. These observations correspond to PS chains becoming less entangled when blended with Ph_8T_8 POSS, which suggests that the Ph_8T_8 POSS molecules are completely dissolved into PS and form a homogeneous solution. The concept of Ph_8T_8 POSS as a good solvent for polystyrene is verified by plotting the normalized plateau modulus, G_N^0 (c) / G_N^0 (1), versus the concentration of solution as depicted in Figure 10. For a good solvent, we expect a power law dependence whose concentration dependent exponent is approximately 2.3 irrespective of the type of solvent in which the polymer chains are present[21]. As shown in Figure 10, the concentration dependent exponent is slightly less than 2.3, thus confirming that the observed viscosity reduction in Ph_8T_8 POSS/PS blends is due to the solvent effect. However, we must point out here that for solutions containing higher than 50 wt% of Ph_8T_8 POSS, we observed a gradual gel-like response with slowly increasing viscosity when the
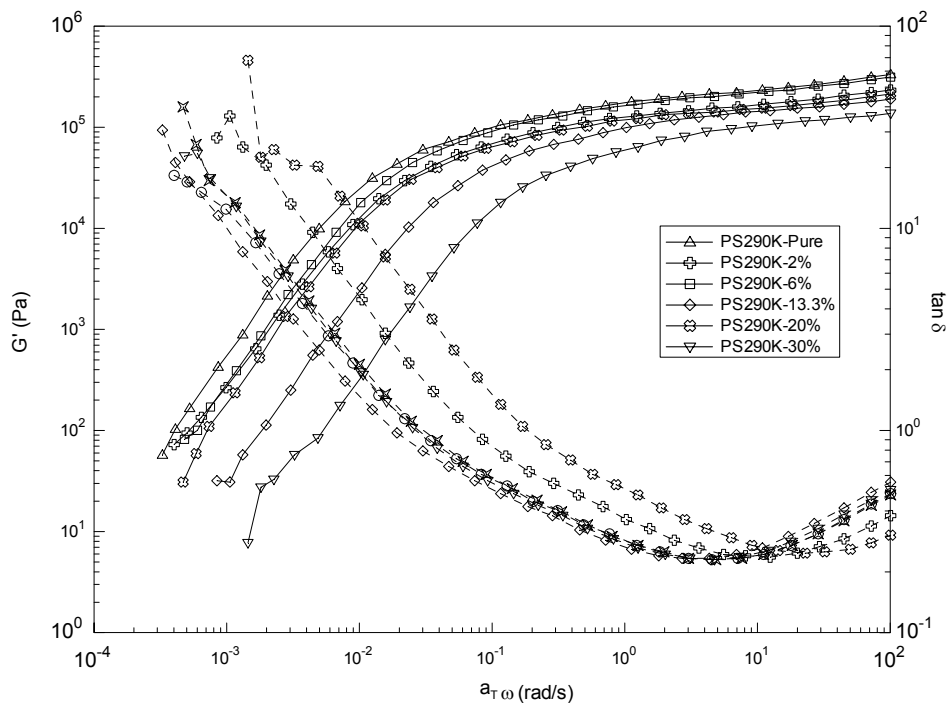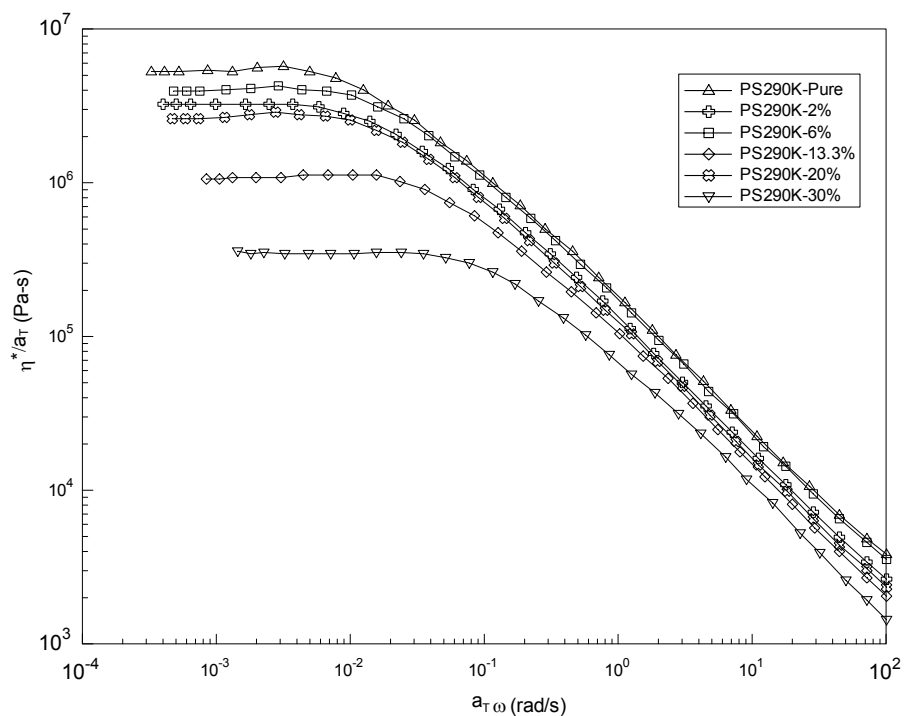
Figure 8(a) Time temperature superposed plots of PS (M_W= 290K Da) and Phenethyl POSS (Ph_8T_8) blends with varying weight fractions of POSS at 150^0C of Storage Modulus ($G^/$) versus reduced frequency ($a_T\omega$)
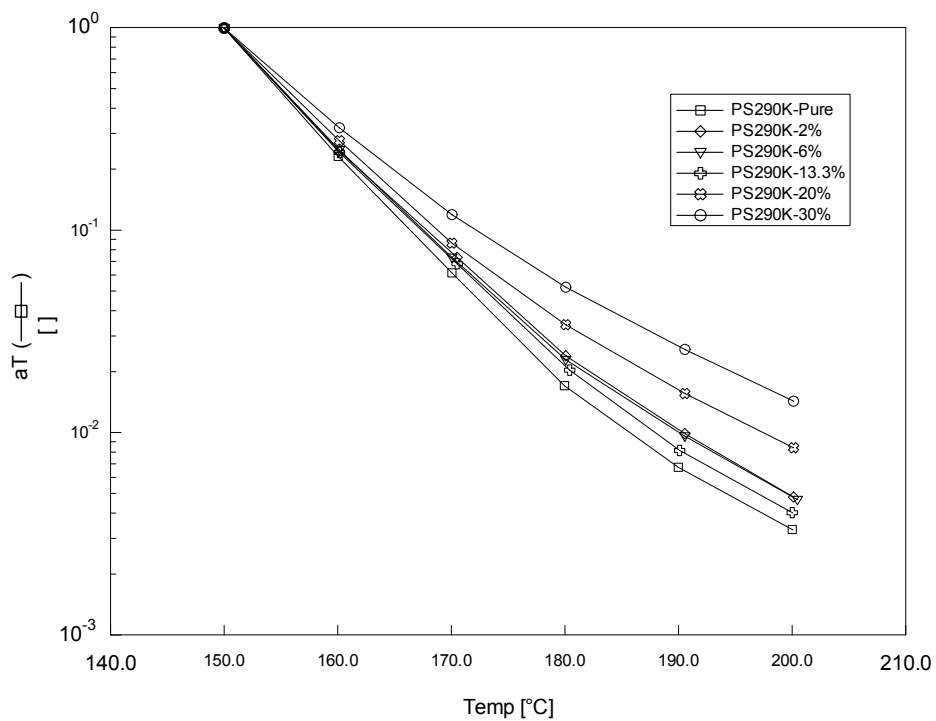
Figure 8(b) Time temperature superposed plots of PS (M_W= 290K Da) and Phenethyl POSS (Ph_8T_8) blends with varying weight fractions of POSS at 150^0C of reduced viscosity (η^*/a_T) versus reduced frequency ($a_T\omega$)

Figure 8(c) Time temperature superposed plots of PS (M_W= 290K Da) and Phenethyl POSS (Ph$_8$T$_8$) blends with varying weight fractions of POSS at 150^0C of shift factors (a_T) versus temperature (Temp)

blend is held isothermally at temperature greater than 100°C. This observation suggests the possibility that Ph_8T_8 POSS undergoes a slow aggregation in the PS matrix. A more detailed investigation on the aggregation kinetic as affected by temperature and the matrix molecular weight is currently being conducted and will be reported in the future.

St_8T_8 POSS / PS Blends

St_8T_8 POSS is used to study the effect of POSS-POSS interactions on the polymer chain dynamics, since it is known that the POSS-POSS interaction in the case of St_8T_8 is greater compared to Ph_8T_8 POSS from the DSC studies. Figure 9(a) is the time-temperature master curves shifted to 150°C for the PS (molecular weight 290K Daltons) blended with different amounts of St_8T_8 POSS. The crossover frequency versus POSS weight fraction and the zero-shear viscosity based on an Ellis model fit were tabulated and are shown in Table 1. The reduced-complex viscosity versus frequency curves for various St_8T_8 POSS fractions are shown in Figure 9(b). Data were shown for the 2%, 6%, 13.3%, 20%, and 30% St_8T_8 POSS blends with 290K PS on the same plot.

In Figure 9(a) the storage modulus curve and the crossover frequency, ω_C, from Table 1 shifts downwards with the addition of St_8T_8 POSS. Although there are some similarities to the effect observed in the case of Ph_8T_8/PS blends, no systemic change on ω_c and G_N^0 were observed. This is in agreement with the DSC results, where no significant T_g depression is observed. We believe this observation can be explained based on the effect of miscibility of St_8T_8 POSS in PS as influenced by a stronger POSS-POSS interaction and the thermorheological behavior of well-dispersed, albeit inert, nano-particulate filled polymer. As discussed previously, the POSS-POSS association is stronger for St_8T_8 POSS as compared to Ph_8T_8 POSS. Consequently, the stronger POSS-POSS interaction affect the miscibility curve of St_8T_8 in PS in
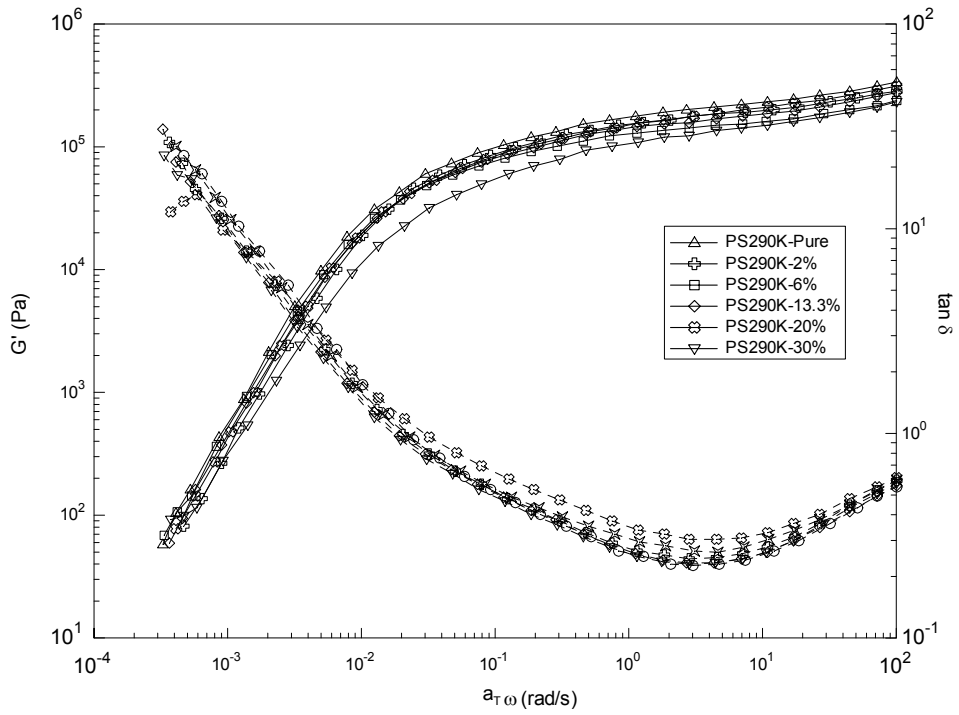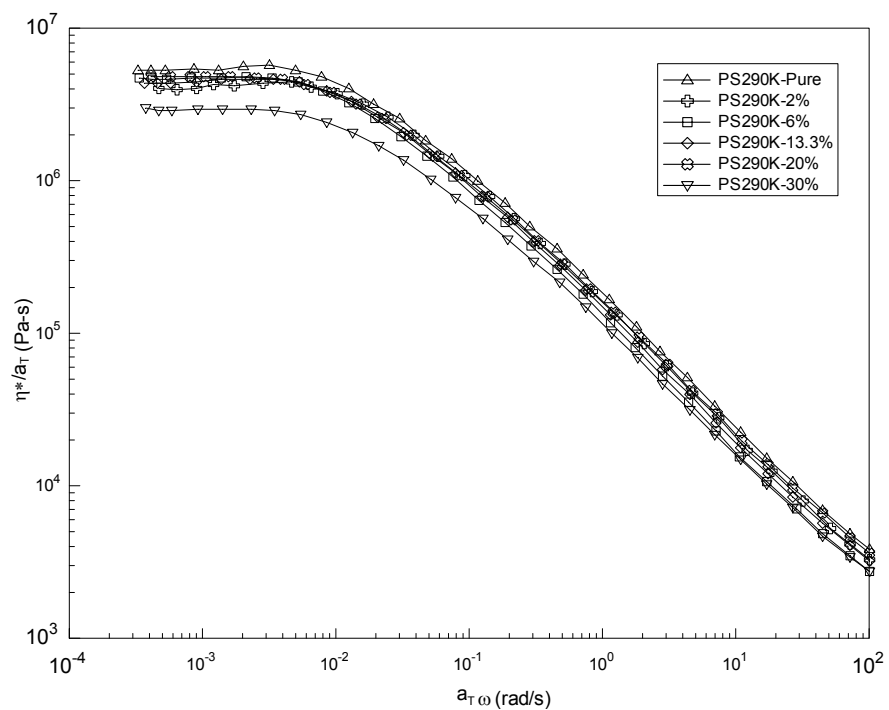
Figure 9(a) Time temperature superposed plots of PS (M_W= 290K Da) and Styrenyl POSS (St_8T_8) blends with varying weight fractions of POSS at 150^0C of storage modulus ($G^/$) versus reduced frequency ($a_T\omega$)

Figure 9(b) Time temperature superposed plots of PS (M_W= 290K Da) and Styrenyl POSS (St_8T_8) blends with varying weight fractions of POSS at 150^0C of reduced viscosity (η^*/a_T) versus reduced frequency ($a_T\omega$)
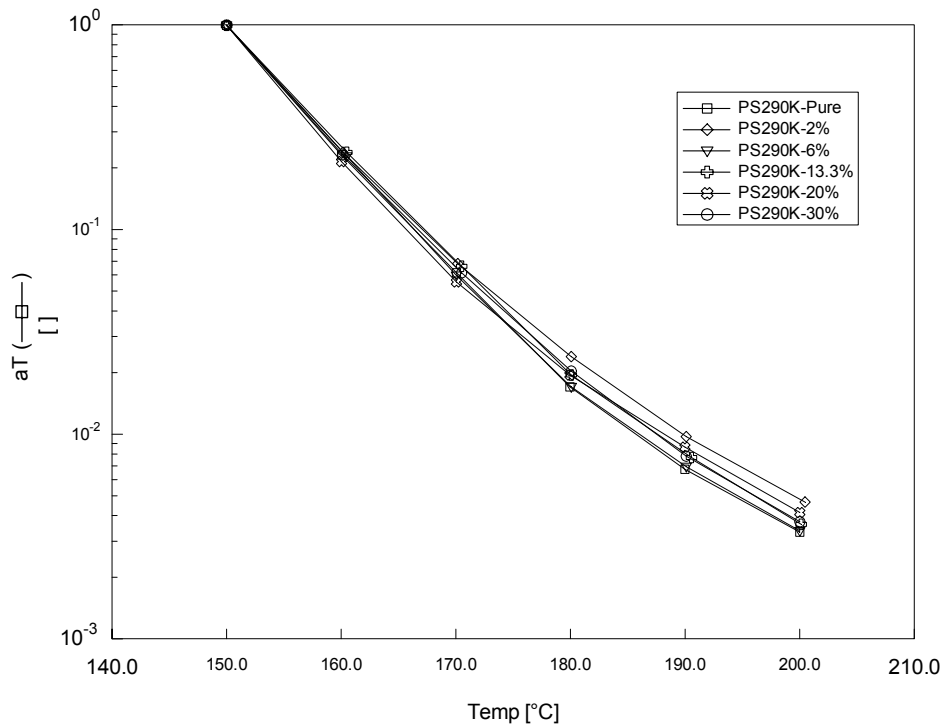
Figure 9(c)

Figure 9c) Time temperature superposed plots of PS (M_W= 290K Da) and Styrenyl POSS (St_8T_8) blends with varying weight fractions of POSS at 150^0C of shift factors (a_T) versus temperature (Temp)
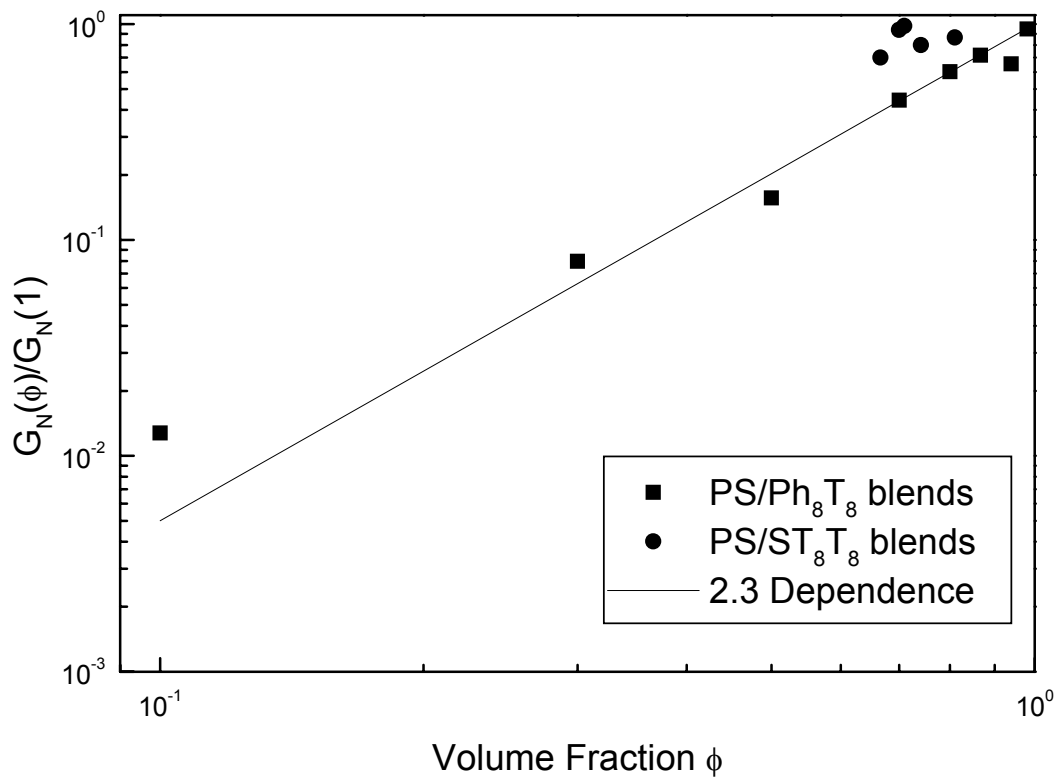
Figure10 Log-Log plot of normalized plateau modulus ($G_N(\phi)/G_N(1)$) versus volume fraction (ϕ)

one POSS-rich and the other polymer-rich, as shown in the TEM images (see Figures 6 and 7). Furthermore, the two-phase morphology remains even with increases in the total POSS concentration. The formation of white drop-like domains can be seen as the dispersed PS domains with lower POSS concentration, where the difference in free energies in both the phases leads to the formation of drops in the homogeneous blend where spinodal decomposition occurs. We believe the droplet domain, which is rich in PS, can reinforce the polymer matrix; thus, the value of the plateau modulus, G_N^0, and ω_c are not strongly affected by the addition of St_8T_8 POSS. Although the value of G_N^0 and ω_c are not strongly affected by the addition of St_8T_8 POSS, we observed a systemic decrease in the value of zero-shear viscosity, $\lim_{\omega \to 0} \eta^*(\omega)$, and the cross-over modulus, $G_c(\omega)$, as amounts of St_8T_8 POSS increased. This is consistent with some other investigations of nano-particle filled polymers[22-24], where the presence of nanoparticles decreased the viscosity of the polymer blend.

Glass Transition Region

The thermomechanical properties of POSS/PS blends in the glassy state was investigated through dynamic thermo-mechanical techniques. Small oscillatory tensile strain at a fixed oscillatory frequency coupled with a simple temperature ramp was applied on films of PS/POSS blends from glassy state through glass transition. The results of the complex elastic modulus, E^*, and the damping factor, $\tan\delta$, for polystyrene blended with varying amount of Ph_8T_8 POSS and St_8T_8 POSS are depicted in Figures 11 and 12, respectively. Figure 11 shows the Ph_8T_8 POSS acting with increasing amount of POSS added in PS. In addition, we also observed a systematic decrease of the glassy state complex elastic modulus with increasing weight fractions of POSS. Coupled with the fact that the $\tan\delta$ peak shifts to lower temperatures due to the plasticization effect, this suggests that the POSS acts as a nanoscopic solvent molecule to PS.
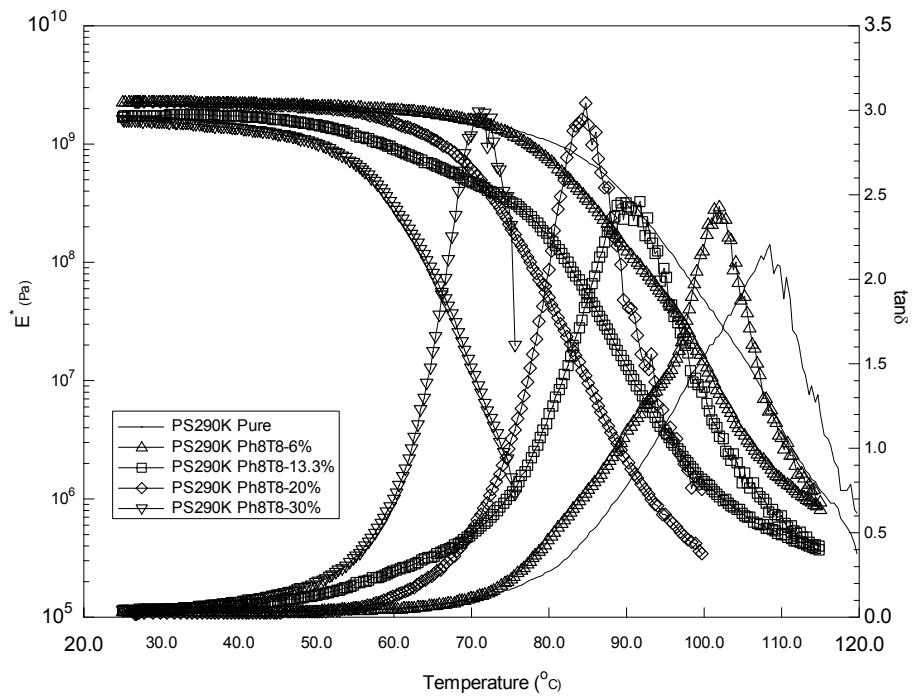
Figure 11 Complex Modulus (E^*) and $\tan\delta$ versus Temperature plot for PS (M_W= 290K Da) and Phenethyl POSS (Ph_8T_8) blends with varying weight fractions of POSS
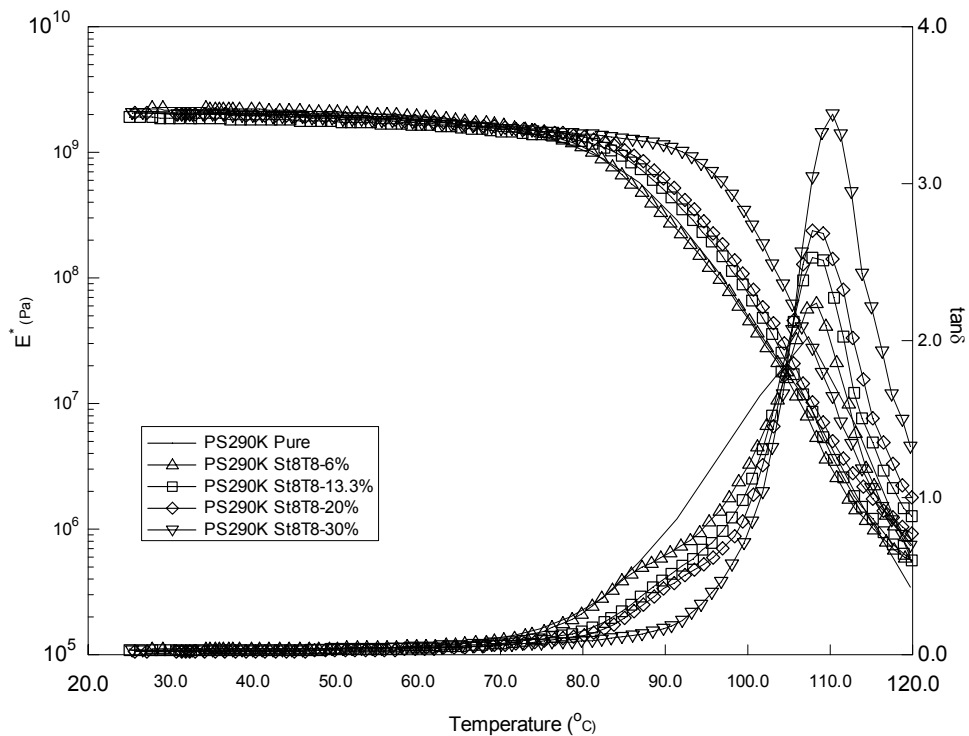
Figure 12 Complex Modulus (E^*) and tanδ versus Temperature plot for PS (M_W= 290K Da) and Styrenyl POSS (St_8T_8) blends with varying weight fractions of POSS

As depicted in Figure 12, the addition of St_8T_8 POSS has a very interesting effect on the glass transition of PS. Although the peak position of the tanδ curve shifts very little with the addition of St_8T_8 POSS, the width of glass transition becomes much sharper with increasing the amount of St_8T_8 POSS. Moreover, the onset of glass transition as determined by the complex elastic modulus curve shows a systematic increase as the weight fraction of St_8T_8 POSS increases.

The glass transition in amorphous polymers is very complex; there have been many papers published in the past 25 years.[25,26] In general, the dynamics of glass transition are controlled by two molecular properties: order and inter-molecular potentials. The influence of inter-molecular potentials on the value of glass transition temperature, T_g, is obvious. Higher inter-molecular binding potentials require more energy input to the material as it undergoes transition from the glassy state to the liquid state, thus leading to higher value of T_g. Similarly, the higher the order in the material, the higher the energy input is needed to achieve a complete "disorder" when material undergoes transition from glass-like to liquid-like behavior. We propose that to accommodate molecularly dispersed, nanoscopic rigid fillers such as St_8T_8 POSS, the local polymeric segment may become more "ordered," which enhances the onset of glass transition temperature. With this increase in the local order, the relaxation spectrum of the polymer chain in the glass transition region becomes narrower, which produces a sharper transition. This local order may persist to the rubbery state, which can facilitate the disentanglement process and leads to the observed reduction in values of $\lim_{\omega \to 0} \eta^*(\omega)$ with St_8T_8 POSS addition.

Conclusions

In this study we have investigated experimentally the effect of POSS macromers when physically blended in entangled PS matrix. The effect on polymer chain dynamics and the phase characteristics by the presence of POSS macromers in PS blends were discussed.

Using DSC, we were able to determine the melting temperature and the heat of fusion for the two POSS molecules, Styrenyl$_8$-POSS (St$_8$T$_8$) and Phenethyl$_8$-POSS (Ph$_8$T$_8$) used in this study. The hydrogenation of styrenyl to phenethyl reduced the melting temperature from 274°C (St$_8$T$_8$ POSS) to 77°C (Ph$_8$T$_8$ POSS), while the heat of fusion remained unchanged (37.7 kJ/mole). In addition, the T$_g$s of all POSS/PS blends used in this study were determined using DSC. No POSS melting peak was observed in all POSS/PS blends used, which suggests the high miscibility between polystyrene and the two POSS molecules used here. The morphologies of the blends were studied by using wide angle X-ray diffraction techniques and TEM. Similar to the DSC observation, X-ray results showed the disappearance of the crystalline nature of POSS when blended with PS, indicating good compatibility. From the TEM images it was clearly observed that dispersion occurs for all weight fractions of POSS in PS. Different phase behavior was achieved depending on the type of POSS used; for Ph$_8$T$_8$ POSS a homogeneous blend was formed because of the lower POSS-POSS interaction, but phase inversion occurred when solid St$_8$T$_8$ POSS macromers were used which have a high binding energy.

Rheological experiments were performed to investigate the influence of POSS addition on the melt dynamics of the polymer chains. We were particularly interested in the influence of well-dispersed, nano-particulate additions on the zero-shear viscosity, $\lim_{\omega \to 0} \eta^*(\omega)$, plateau modulus, G_N^0 and the cross-over frequency, ω_C of polymer melts.

In the Ph$_8$T$_8$ POSS/PS blends, because of the low POSS-POSS interaction, any POSS interactions are screened out by the presence of PS. Ph$_8$T$_8$ POSS/PS blend forms a homogeneous

solution. The rheological responses of these blends are the same as if a good solvent was added to PS. We observed a systemic decrease in the zero-shear viscosity, plateau modulus, cross-over frequency as the concentration of Ph_8T_8 POSS increased, as shown in Table 1.

For St_8T_8 POSS/PS blends, due to a stronger POSS-POSS association, the blend forms a two-phase morphology. Regardless of the concentration of St_8T_8 POSS in PS, the POSS-rich domain forms a continuous phase and PS-rich domain as the discontinuous phase. As we increased the concentration of St_8T_8 POSS, only the PS-rich discontinuous phase was increased. Since St_8T_8 POSS is molecularly dispersed in PS, the zero shear viscosity of the blends decreases with the addition of St_8T_8 POSS, which is similar to that observed in the case of Ph_8T_8/PS blends (shown in Table 1). However, due to persistence of the two-phase morphology, no systematic changes in ω_c and G_N^0 were observed with increasing concentration of POSS, since phase behavior controls the rheological behavior of these blends.

Thermomechanical properties of POSS/PS blends in the glassy state were investigated through dynamic thermo-mechanical techniques. Small oscillatory tensile tests on the Ph_8T_8/PS blend films showed a gradual decrease in glass transition temperature and elastic modulus with increasing concentration, which further confirmed the plasticization theory. In the case of St_8T_8 POSS/PS blends, not much variation in glass transition temperature was observed, which supports the DSC data; however, the width of glass transition became much sharper with increasing amounts of St_8T_8 POSS. Moreover, the onset of glass transition as determined by the complex elastic modulus curve showed a systematic increase as the weight fraction of St_8T_8 POSS increased. Due to the higher order in the St_8T_8 POSS as observed from DSC, when St_8T_8 POSS/PS blends undergo a transition from glass-like to liquid-like behavior we propose that the addition of molecularly dispersed, nanoscopic rigid fillers such as St_8T_8 POSS, the local

polymeric segment may become more "ordered," which enhances the onset of the glass transition.

POSS nanoparticles which are compatible with the polymer chains could be used to lower the free energy of the polymer mixture and also reduce the viscosity of a polymer mixture as a plasticizer. Though miscibility and aggregation kinetics could be controlled in these types of nanocomposites, since the chemistry of POSS particles can be modified depending on the system to be used, it should be noted that restrictions on the organic pendant group on the silsesquioxane cage plays an important role in governing the dynamics of systems involving POSS.

Acknowledgment

References

1. Ning, Y.P.; Tang, M.Y.; Jiang, C.Y.; Mark, J.E. and Roth, W.C.; J Appl. Polym. Sci., **29**, 3209, (1984).

2. Kojima, Y.; Usuki, A.; Kawasumi, M.; Okada, A.; Kurauchi, T. and Kamigaito, J.; J. Polym. Sci: Part A: Polym. Chem., **31**, 983, (1993).

3. Wang, M.S. and Pinnavaia, T.J.; Chem. Mat., **6**, 468, (1994).

4. Lichtenhan, J.D.; Comments Inorg. Chem., **17**, 115, (1995)

5. Asakura, S. and Oosawa, F.; J. Chem. Phys., **22**, 1255 (1954)

6. Vrij, A.; Pure & Appl. Chem., **48**, 471 (1976).

7. de Gennes, P.G.; "Scaling Concepts in Polymer Physics", Cornell University Press, (1979).

8. Sear, R.P.; J. Chem. Phys., **115**, 575 (2001).

9. Eisenriegler, E.; Hanke, A. and Dietrich, S.; Phys. Rev. E, **54**, 1134 (1996).

10. Hanke, A.; Eisenriegler, E. and Dietrich, S.; Phys. Rev. E, **59**, 6853, (1999).

11. Eisenriegler, E.; J. Chem. Phys., **113**, 5091 (2000).

12. Maassen, R.; Eisenriegler, E. and Bringer, A.; J. Chem. Phys., **115**, 5292 (2001).

13. Meijer, E.J. and Frenkel, D.; J. Chem. Phys., **100**, 6873 (1994).

14. Louis, A.A.; Bolhuis, P.G.; Meijer, E.J. and Hansen, J.P.; J. Chem. Phys., **117**, 1893 (2002).

15. Fuchs M. and Schweizer, K.S.; Europhys Lett., **51**, 621 (2000).

16. Fuchs M. and Schweizer, K.S.; J. Phys: Cond. Matter, **14**, 239 (2002).

17. Jansons, K.M. and Philips, C.G.; J. Colloid Interface Sci., **137**, 75 (1990).

18. Odijk, T.; J. Chem. Phys., **106**, 3402 (1997).

19. Odijk, T.; Physica A, **278**, 347 (2000).

20. Blanski, R.L.; Lee, A.; Geng, H.P.; Phillips, S.H.; Chaffee, K. and Lichtenhan, J.L.; Polym. Preprint, **41**, 585 (2001).

21. Rubinstein M. and Colby R.H; "Polymer Physics", Oxford University Press, (2003).

22. Starr, F. W.; Schroeder, T. B. and Glotzer, S. C.; Phys. Rev. E, **64**, 021802 (2001).

23. Starr, F. W.; Schroeder, T. B. and Glotzer, S. C.; Macromolecules, **35**, 4481 (2002).

24. Mackay, M.E.; Dao T.T.; Tuteja, A.; Ho, D.L.; Van Horn, B.; Kim, H.C. and Hawker, C.J.; Nature Materials, **2**, 762 (2003).

25. Donth, R.J.; "Relaxation and Thermodynamics in Polymers-Glass Transition", Akademie Verlag, Berlin, (1992).

26. Larson, R.G.; Chapter 4 of "The Structure and Rheology of Complex Fluids", Oxford University Press, (1999).

Figures

1. DSC plot of Phenethyl POSS (Ph_8T_8) and PS (M_W= 290K Da) / Phenethyl POSS 30%wt blend

2. DSC plot of Styrenyl POSS (St_8T_8) and PS (M_W= 290K Da) /Styrenyl POSS 30%wt blend

3. X-Ray plot of Phenethyl POSS (Ph_8T_8) and PS (M_W= 290K Da) / Phenethyl POSS 20%wt blend

4. X-Ray plot of Styrenyl POSS (St_8T_8) and PS (M_W= 290K Da) /Styrenyl POSS 20%wt blend

5. TEM Image of PS (M_W= 2M Da)/ Phenethyl POSS blend (50 wt% POSS)

6. TEM Image of PS (M_W= 2M Da)/ Styrenyl POSS blend (20 wt% POSS)

7. TEM Image of PS (M_W= 2M Da)/ Styrenyl POSS blend (50 wt% POSS)

8. Time temperature superposed plots of PS (M_W= 290K Da) and Phenethyl POSS (Ph_8T_8) blends with varying weight fractions of POSS at 150^0C a) Storage Modulus ($G^/$) versus Reduced frequency ($a_T\omega$) b) Reduced viscosity ($\eta^*_{/}\,a_T$) versus Reduced frequency ($a_T\omega$) c) Shift factors (a_T) versus Temperature (Temp)

9. Time temperature superposed plots of PS (M_W= 290K Da) and Styrenyl   POSS (St_8T_8) blends with varying weight fractions of POSS at 150^0C a) Storage Modulus ($G^/$) versus Reduced frequency ($a_T\omega$) b) Reduced viscosity ($\eta^*_{/}\,a_T$) versus Reduced frequency ($a_T\omega$) c) Shift factors (a_T) versus Temperature (Temp)

10. Log-Log plot of Normalized Plateau Modulus ($G_N\,(\phi)/G_N\,(1)$) versus Volume fraction (ϕ)

11. Complex Modulus (E^*) and $\tan\delta$ versus Temperature plot for PS (M_W= 290K Da) and Phenethyl POSS (Ph_8T_8) blends with varying weight fractions of POSS

12. Complex Modulus (E^*) and $\tan\delta$ versus Temperature plot for PS (M_W= 290K Da) and Styrenyl POSS (St_8T_8) blends with varying weight fractions of POSS